

Poster session 7: Steel structures

Objektyp: **Group**

Zeitschrift: **IABSE congress report = Rapport du congrès AIPC = IVBH
Kongressbericht**

Band (Jahr): **12 (1984)**

PDF erstellt am: **24.09.2024**

Nutzungsbedingungen

Die ETH-Bibliothek ist Anbieterin der digitalisierten Zeitschriften. Sie besitzt keine Urheberrechte an den Inhalten der Zeitschriften. Die Rechte liegen in der Regel bei den Herausgebern.

Die auf der Plattform e-periodica veröffentlichten Dokumente stehen für nicht-kommerzielle Zwecke in Lehre und Forschung sowie für die private Nutzung frei zur Verfügung. Einzelne Dateien oder Ausdrucke aus diesem Angebot können zusammen mit diesen Nutzungsbedingungen und den korrekten Herkunftsbezeichnungen weitergegeben werden.

Das Veröffentlichen von Bildern in Print- und Online-Publikationen ist nur mit vorheriger Genehmigung der Rechteinhaber erlaubt. Die systematische Speicherung von Teilen des elektronischen Angebots auf anderen Servern bedarf ebenfalls des schriftlichen Einverständnisses der Rechteinhaber.

Haftungsausschluss

Alle Angaben erfolgen ohne Gewähr für Vollständigkeit oder Richtigkeit. Es wird keine Haftung übernommen für Schäden durch die Verwendung von Informationen aus diesem Online-Angebot oder durch das Fehlen von Informationen. Dies gilt auch für Inhalte Dritter, die über dieses Angebot zugänglich sind.



POSTER SESSION 7

Steel Structures

Structres métalliques

Stahltragwerke

Coordinator: R.S. Stilwell, Canada

Installation for Runnability on Long Span Bridge

Akira TAKAYAMA, Hiroaki TSURUTA
 Mitsuru GOTO, Eiji KATAYAMA
 Honshu-Shikoku Bridge Authority
 Tokyo, Japan

Runnability of Train on Transit Girder System.

For development of transit girder system, runnability of train had been studied as mentioned below.

Runnability of trains at the transit girder system can be separately checked for sections of the expansion joint and the dispersion system for angular bend.

At the expansion joint, the structure is designed so that rail tracks may continue to secure a proper gauge line and wheelset load can be structurely supported.

Rail of the inserted girder type expansion joint is cut out partially to keep space for expansion, and the guardrails are arranged to prevent derailment.

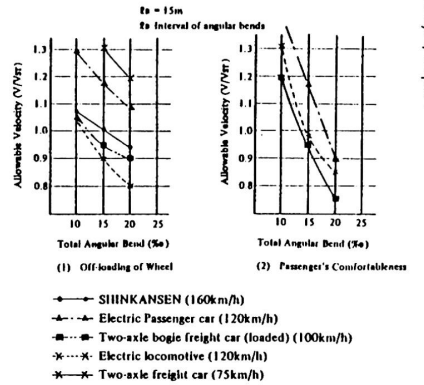
For the runnability on the expansion joint, running tests by actual cars were conducted in 1974 to certify safety of trains with speed up to 180 km/hr.

The runnability on the angular bend section is extremely influenced by a vertical and horizontal angular bend. The safety against derailment when a train run on the transit girder with vertical, horizontal angular bend or composite angular bend of the both and passenger's comfortableness for vertical and horizontal vibration had to be investigated.

The investigations for derailment and comfortableness were carried out for criteria of the rate of off-loading of wheels and the lateral pressure and magnitude of the vibration, respectively, and they were numerically analyzed or simulated for various types of cars.

And, important items among them were confirmed by running tests of actual cars and model cars, and results of the running tests and the calculation were compared. As the result of these investigations, relation between the running speed and the limit of angular bend is established as shown in right figure.

For example, when the total angular bend is 10‰ and span of the dispersion girder is 15m, these figures show that allowable velocity (V/V_{Sr}) of Shinkansen is 1.07 for the rate of off-loading of wheels, in other words, Shinkansen car can run with 1.07 times speed of standard running speed. As for an electric locomotive, it can run with 1.04 times speed of 120 km/hr.



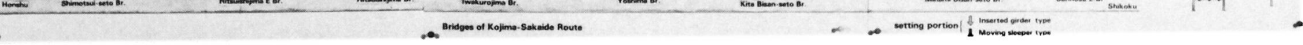
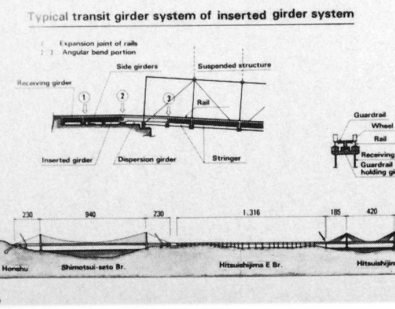
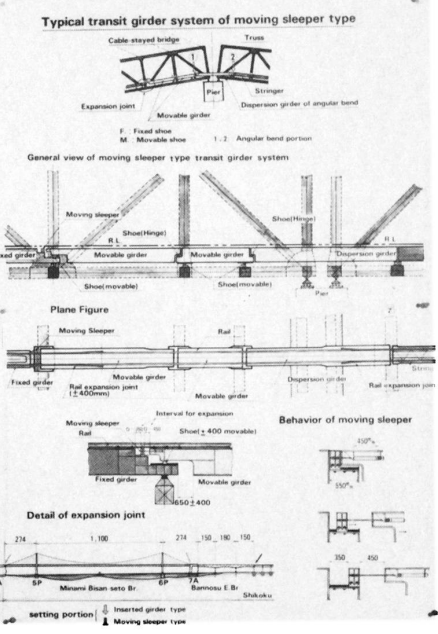
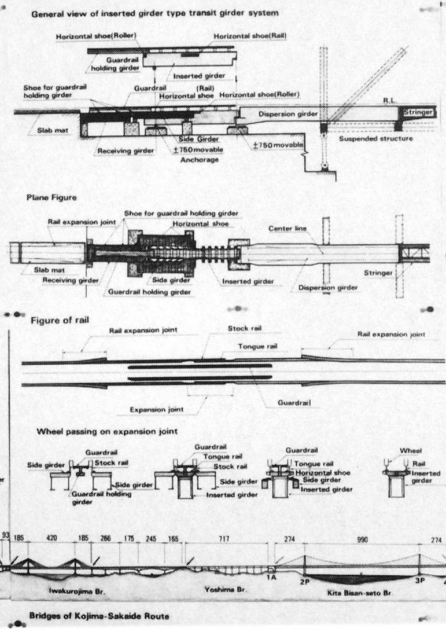
Allowable velocity V/V_{Sr} above is defined as the ratio of investigated result to standard running speed

Fig.

Allowable speed of various types of cars

INSTALLATION FOR RUNNABILITY ON LONG-SPAN BRIDGE

In Kojima-Sakaide Route of Honshu-Shikoku Bridge Project, suspension bridges and cable stayed bridges which have high flexibility are being constructed for highway and railroad with high speed trains. At the end of these bridges, large amount of expansion/contraction and angular bend occur. In order to let the high speed train run safely on these deformation, transit girder system has been developed. Two types of expansion joint are developed. One is called the inserted girder type for expansion (including effect of earthquake) up to ± 750 mm of suspension bridges. And, another is called the moving sleeper type for expansion up to ± 400 mm of cable stayed bridges.





Beam to-Column-Connections with Composite Beams

Hiroshi OSANO
Res. Assoc.
Tokyo Denki Univ
Tokyo, Japan

Masami NAKAO
Prof. Dr.
Tokyo Denki Univ.
Tokyo, Japan

Sanzo UNNO
Prof. Dr.
Tokyo Denki Univ.
Tokyo, Japan

Takeo NAKA
Prof. emeritus
Univ. of Tokyo
Tokyo, Japan

This research deals with the contribution of reinforced concrete slab of composite beams on the strength and the deformation capacity of steel beam-to-column connections subjected to seismic loading.

Dimension and configuration of specimens are shown in figure 1 and table 1. Relative yield strength of panel-zone to that of adjoining members is expressed marks "Rpy" and "sRpy" in table 1. Those are considered to be the key parameter on the evaluations of strength, deformation capacity and energy absorption of beam-to-column connections.

Figures 4a-4c are the summary of representative relations between load and shear deformation of panel-zone. Vertical axis represents the ratio of load to calculated yield strength of beam-to-column connection composed of bare steel beams and column, while horizontal axis represents the ratio of shear deformation of panel-zone to calculated yield shear deformation. Dotted lines in figures 4a-4c show the test results of beam-to-column connections of the same configuration without concrete slab. The reinforcing effect of steel beam-to-column connections by the reinforced concrete slabs of composite beam is illustrated.

A model to take the effect of concrete slab into consideration is proposed in figure 5. In this model, the strength of panel-zone is considered to increase by the enlargement of nominal volume of panel-zone as shown in the figure 5. Relation between "sRpy" (relative yield strength of panel-zone to that of adjoining steel members) and strength, deformation capacity and energy absorption are shown in figures 6a-6d with the other test results of beam-to-column connections composed of bare steel beams and column. The empirical formulas in figures 6a-6d are obtained by regression analyses on the test results of beam-to-column connections composed of bare steel beams and column. Shiftings to the estimated results of yield strength of enlarged panel-zone are indicated by arrows. The seismic behavior of steel beam-to-column connections with composite beams can be evaluated by making use of the model in figure 5 and empirical formulas in figures 6a-6d.

BEAM-TO-COLUMN CONNECTIONS WITH COMPOSITE BEAMS

Table 1 Specimens

No.	Specimen	Column	Beam	Slab type	R _{py}	sR _{py}
1	Z0-I	H-300x300x22x22	H-350x175x9x12	I	1.13	0.80
2	A0-I	H-300x300x16x16	H-350x175x9x12	I	0.63	0.62
3	B'0-I	H-250x250x12x16	H-350x175x9x12	I	0.56	0.40
4	B'0-III	ditto	ditto	III	0.56	0.40
5	B'1-I	ditto	ditto	I	0.49	0.80
6	C0-I	H-250x250x 9x16	H-350x175x9x12	I	0.33	0.33
7	C0-IIW	ditto	ditto	IIW	0.51	0.33
8	C0-IIS	ditto	ditto	IIS	0.28	0.33

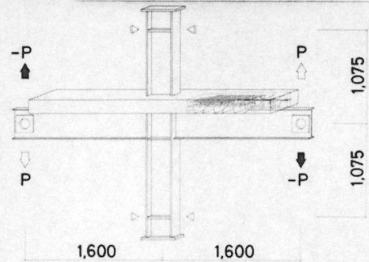


Fig. 1 Configuration of Specimens

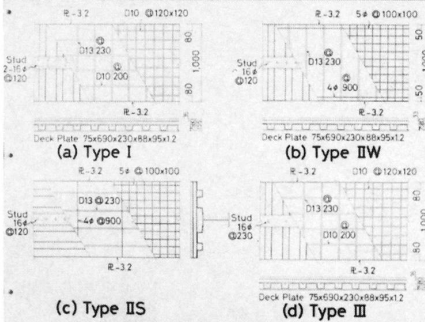


Fig. 2 Details of Concrete Slabs

$R_{py} = P/P_y$ $sR_{py} = sP_y/P_y$ $\mu_{20} = \delta_{20}/\delta_y$ $E_{20} = sP_{20}^C \times \delta_y^2$
 P_y : Yield load of panel-zone
 P_u : Ultimate strength of frame subassemblage
 P_{20} : Yield load of adjoining members, whichever is smaller
 sP_{20} : Yield load of adjoining steel members, whichever is smaller
 δ_y : Yield deformation of frame subassemblage

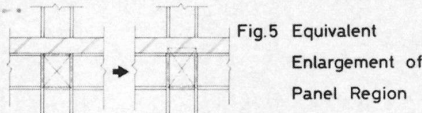


Fig. 5 Equivalent Enlargement of Panel Region

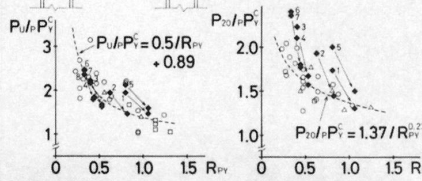


Fig. 6a $P_u/P_y - R_{py}$ Relation Fig. 6b $P_{20}/P_y - R_{py}$ Relation

(P, E)₂₀: At a point where shear deformation of panel-zone became twenty times the yield shear deformation.

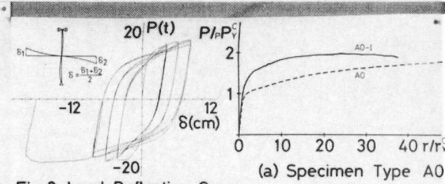


Fig. 3 Load-Deflection Curve (a) Specimen Type A0

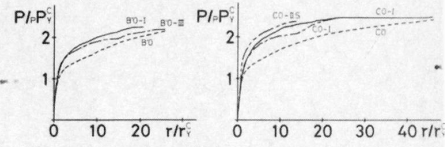


Fig. 4 Load-Shear Deformation Curves (b) Specimen Type B'0 (c) Specimen Type C0

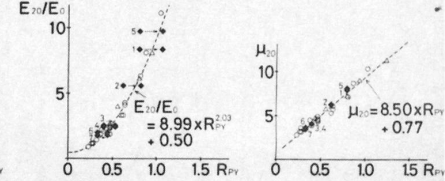


Fig. 6c $E_{20}/E_{20} - R_{py}$ Relation Fig. 6d $\mu_{20} - R_{py}$ Relation

E_{20} : Absorbed energy of frame subassemblage
 δ : Deformation of frame subassemblage shown in Fig. 3



Optimum Design of Double-Layer Space Grids

Henning AGERSKOV

Assoc. Prof. of Struct. Eng.
Technical University of Denmark
Lyngby, Denmark

In recent years extensive and increasing use has been made of space trusses, especially in the form of double-layer space grids. These types of structures have in many cases been able to compete with more traditional constructions. The main areas of application have been sports halls, swimming pools, exhibition buildings, churches, shopping centres, hangars, factory buildings, etc., where the space grid is used as roof construction.

In the design, almost unlimited possibilities exist in practice for the choice of geometry of space trusses. This forms the background for a research project, in which the optimum design of double-layer space grids has been investigated. As a first part of the investigation, a study covering what has, until recently, been obtained as regards optimization of double-layer space grids was carried out. With the results of this investigation as a starting point, various geometrical designs were studied in detail to determine the optimum design. Both square and rectangular grids have been investigated, under the assumption of either simple supports along the entire edge or column supports at the corners.

In determination of the optimum design, an ordinary mathematical optimization based on a minimum of material consumption, was found to be of little practical interest. The present investigation is based on assumptions concerning nodes, members, supports, loading, etc., which make the results realistic to a practical design. To determine the optimum de-

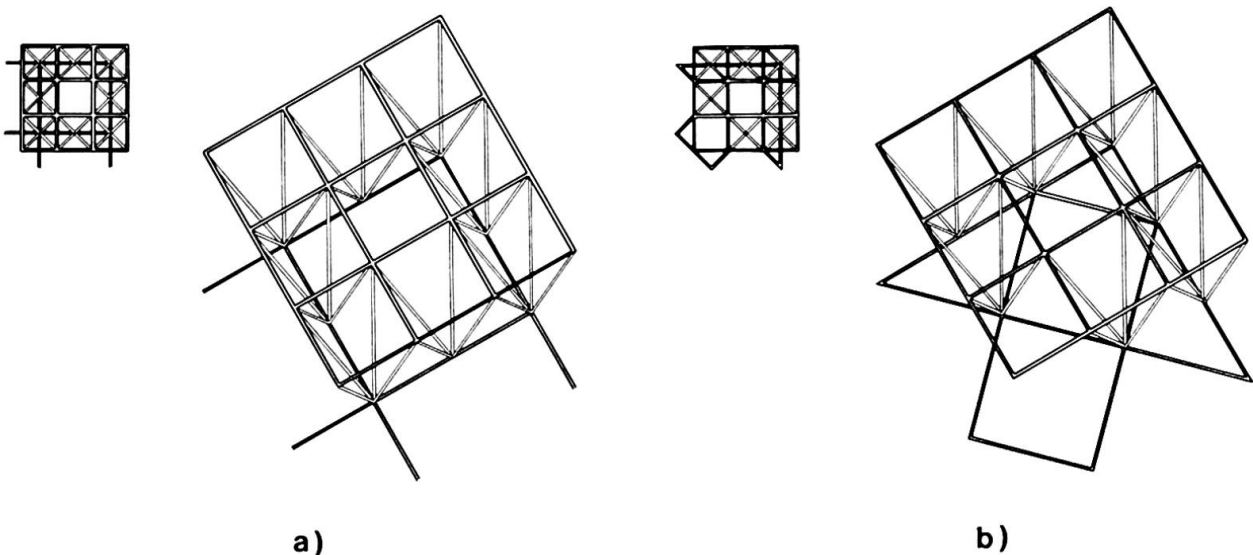


Fig. 1. Space grid systems, which will in general result in good overall economy.



sign, both the material consumption, the number of nodes, and the number of members in the structure have to be considered, while an optimum design based only on a minimum of material will rarely, if ever, be an economical optimum for a double-layer space grid.

On the basis of the results obtained in the investigation, guidelines for the structural engineer to obtain an optimum design, have been worked out. Guidelines are given for choice of overall geometry of simply supported and corner-supported square and rectangular space grids.

RECOMMENDATIONS

The following general recommendations concerning optimum design of double-layer space grids can be made:

1. The member density must be small. In addition to giving a small material consumption, this leads to a grid with relatively few nodal points and thus least possible production costs for nodes, erection expenses, etc.
2. The system should be chosen so that the space grid is built of relatively long tension members and relatively short compression members.
3. For rectangular, relatively long space grids, optimum design is obtained with systems where the load is mainly carried across the short span. Systems where the members in both top and bottom layer grids are parallel to the edges will generally result in the least material consumption.
4. If both the material consumption and the number of nodes and number of members are considered, the space grid systems shown in Fig. 1 a and b will, generally speaking, result in good overall economy. This could be concluded from investigations on both square and rectangular double-layer space grids, simply supported along the entire edge or column-supported at the corners.

REFERENCES

1. Agerskov, H., and Gudjonsson, H., "Optimal udformning af rumgitterkonstruktioner", Proceedings of the Scandinavian Conference on Steel Research, Copenhagen, Denmark, Aug., 1979, pp. VI. 5.1-13.
2. Agerskov, H., "Optimum Design of Double-Layer Space Trusses", Report, Dept. of Civil-Structural Engineering, Portland State University, Portland, Or., U.S.A., 1981.
3. Agerskov, H., and Bjørnbak-Hansen, J., "Optimum Design of Corner-Supported Double-Layer Space Trusses", Report No. R 177, Dept. of Structural Engineering, Technical University of Denmark, Lyngby, Denmark, 1983.
4. Agerskov, H., "Optimum Design of Double-Layer Space Grids", Dept. of Structural Engineering, Technical University of Denmark, Lyngby, Denmark, Sept., 1984, 21 pp.

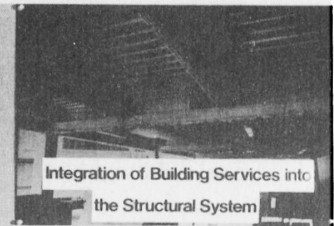
STUB-GIRDER FLOOR SYSTEM



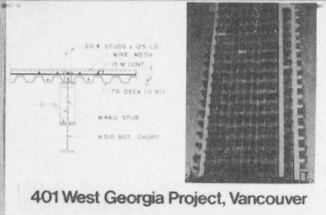
Full Scale Test Program at the University of Saskatchewan



Stub-Girder Floor System



Integration of Building Services into the Structural System



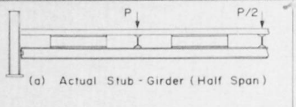
401 West Georgia Project, Vancouver

ADVANTAGES:
 Integration of Building Services
 Simplified Girder to Beam Connection
 Reduced Building Heights, Lower Costs

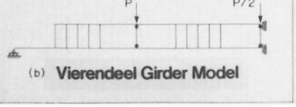
APPLICATIONS IN CANADA:

Building	Storeys	Area (m ²)
Nova Building, Calgary	37	70,000
Manulife Bldg., Edmonton	24	71,000
401 West Georgia Project, Vancouver	22	28,000

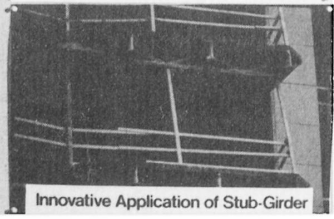
ANALYSIS
 Most Common Method of Analysis is to Model the Stub-Girder as a Vierendeel Girder and Then Use a Conventional Stiffness Program



RESEARCH
 Univ. of Saskatchewan, Saskatoon, Canada
 Univ. of Alberta, Edmonton, Canada
 Louisiana State Univ., Baton Rouge, U.S.A.
 Univ. of Arizona, Tucson, U.S.A.

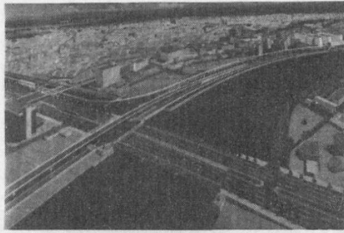


Failure Mechanism Observed

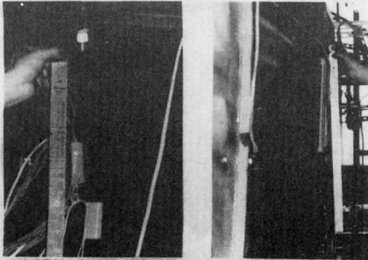


Innovative Application of Stub-Girder

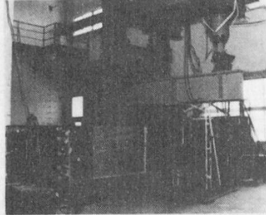
ULTIMATE STRENGTH OF HIGH DEPTH CURVED GIRDER



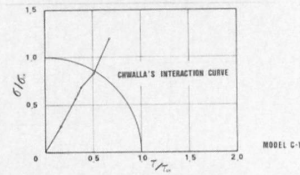
AIR VIEW FUTURE OKINAWA CITY MONO-RAIL WHICH WILL BE COMPLETED IN 1987. THE PURPOSE OF THIS STUDY IS TO INVESTIGATE THE BEHAVIOR OF THE CURVED GIRDERS TO BE CONSTRUCTED WHERE THE GIRDERS ARE DESIGNED WITH THE RADIUS OF 55 M TO 120 M.



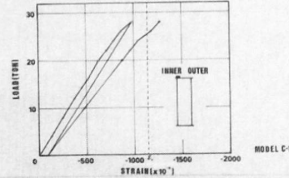
LOCAL BUCKLING OF INNER WEB PLATE & DEFORMATION AT OUTER SIDE MODEL C-1



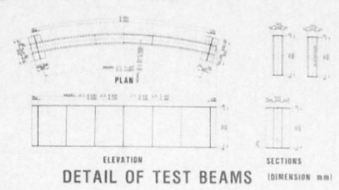
SET-UP OF TEST BEAM MODEL C-1



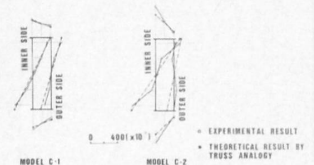
RELATIONSHIP BETWEEN RATIOS σ_{1cr} AND τ_{1cr}



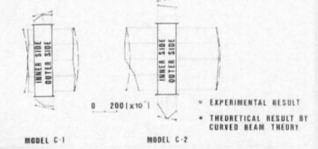
LOAD-LONGITUDINAL STRAIN RELATIONSHIP



DETAIL OF TEST BEAMS



LONGITUDINAL STRAIN DISTRIBUTIONS AT MIDSPAN (10 TONS MIDSPAN LOADING)



SHEAR STRAIN DISTRIBUTION AT 500 mm FROM SUPPORT (10 TONS MIDSPAN LOADING)

Leere Seite
Blank page
Page vide